



Cite this: DOI: 10.1039/c5cp00250h

# Relating voltage and thermal safety in Li-ion battery cathodes: a high-throughput computational study†

Anubhav Jain,‡ Geoffroy Hautier,§ Shyue Ping Ong,¶ Stephen Dacek and Gerbrand Ceder\*

High voltage and high thermal safety are desirable characteristics of cathode materials, but difficult to achieve simultaneously. This work uses high-throughput density functional theory computations to evaluate the link between voltage and safety (as estimated by thermodynamic O<sub>2</sub> release temperatures) for over 1400 cathode materials. Our study indicates that a strong inverse relationship exists between voltage and safety: just over half the variance in O<sub>2</sub> release temperature can be explained by voltage alone. We examine the effect of polyanion group, redox couple, and ratio of oxygen to counter-cation on both voltage and safety. As expected, our data demonstrates that polyanion groups improve safety when comparing compounds with similar voltages. However, a counterintuitive result of our study is that polyanion groups produce either no benefit or reduce safety when comparing compounds with the same redox couple. Using our data set, we tabulate voltages and oxidation potentials for over 105 combinations of redox couple/anion, which can be used towards the design and rationalization of new cathode materials. Overall, only a few compounds in our study, representing limited redox couple/polyanion combinations, exhibit both high voltage and high safety. We discuss these compounds in more detail as well as the opportunities for designing safe, high-voltage cathodes.

 Received 15th January 2015,  
Accepted 20th January 2015

DOI: 10.1039/c5cp00250h

www.rsc.org/pccp

## Introduction

Voltage and thermal safety are important design considerations for Li ion battery cathode chemistries. A high voltage improves energy density and power delivered by the battery; however, high voltage cathodes must also maintain safe operation of the cell. Indeed, a history of fires,<sup>1</sup> from laptops to cars to aboard a 'Dreamliner' aircraft,<sup>2</sup> has renewed focus towards designing safer Li ion batteries.<sup>3,4</sup>

While many components of a battery are responsible for the overall thermal safety of a battery (henceforth referred to simply as safety), a cathode material's safety is generally assessed as its resistance to releasing O<sub>2</sub> at elevated temperatures in its

charged state. Released oxygen can combust the organic electrolyte and eventually lead to thermal runaway of the cell and fire.<sup>3,5,6</sup>

To design the next generation of safe, high-voltage cathodes, the research community has typically targeted polyanion chemistries.<sup>7,8</sup> Polyanion-based cathodes, which include phosphates, silicates, borates, and sulfates, are known to exhibit higher voltages through the inductive effect.<sup>9,10</sup> Polyanions are also thought to guard against O<sub>2</sub> release by embedding the oxygen atoms within a polyanion group such as PO<sub>4</sub> or SiO<sub>4</sub> that is speculated to be difficult to disrupt.<sup>11–14</sup> The well-known LiFePO<sub>4</sub> material is one example of a polyanion-based cathode that exhibits a fairly high voltage (3.5 V) while also possessing good safety characteristics.<sup>15,16</sup> However, it has now been demonstrated that not all phosphates are resistant to O<sub>2</sub> release; for example, charged LiCoPO<sub>4</sub> (4.5 V) readily releases O<sub>2</sub> even at low temperatures.<sup>17</sup>

In distinguishing safe and unsafe cathodes, previous work by Godshall *et al.* has indicated that high voltage cathodes are more prone to O<sub>2</sub> release.<sup>18</sup> They report that the equilibrium oxygen pressure of a cathode is independent of chemistry and increases linearly with voltage.<sup>18</sup> However, there exist three major limitations with this study. The first is that voltages were measured at equilibrium, which pertains only to conversion cathodes. Nearly all commercially relevant rechargeable batteries are based on insertion cathodes, which is the subject of our study.

Department of Materials Science & Engineering, Massachusetts Institute of Technology, Cambridge, Massachusetts, 02139, USA. E-mail: gceder@mit.edu; Tel: +1-617-253-1581

† Electronic supplementary information (ESI) available. See DOI: 10.1039/c5cp00250h

‡ Present address: Environmental Energy & Technologies Division, Lawrence Berkeley National Laboratory, Berkeley, California, 94720, USA.

§ Present address: Institute of Condensed Matter and Nanosciences, Université catholique de Louvain, Louvain-la-Neuve, Belgium.

¶ Present address: Department of Nanoengineering, University of California San Diego, La Jolla, California 92093, USA.

Second, the data pre-dates most investigations of polyanion-based cathodes and is reported only for three similar Li metal oxide systems. Finally, measurements were only performed at very low voltages ( $<1.81$  V) due to electrolyte limitations of the time. Recently, Huggins has re-examined the same data set to extrapolate their linear relation to higher voltages and ambient temperatures, finding that cathodes higher than 3 V should become prone to  $O_2$  release.<sup>19</sup> However, like the earlier study the data used to make this claim is limited only to three lithium metal oxide conversion systems at very low voltages. Therefore, the broad claim that chemistry does not affect the relation between voltage and oxygen pressure merits further investigation using an expanded test set that includes polyanion systems and uses insertion voltages that are more representative of today's battery materials.

In previous works, we have introduced computational methods for evaluating both voltage and oxidation potential based on density functional theory (DFT) calculations.<sup>20–24</sup> The voltage is computed for Li insertion (out-of-equilibrium behavior) and closely matches experimental values.<sup>25,26</sup> The oxidation potential is determined by computing phase stability diagrams analogously to the experimental approach of Godshall *et al.*<sup>18</sup> A major advantage of the computational approach is that it can rapidly characterize diverse chemical systems within a high-throughput framework,<sup>27,28</sup> allowing us to assess statistical trends in safety over a variety of oxides and polyanions.

Using such computations, we previously reported the thermal instability of charged  $LiMnPO_4$  cathodes compared to charged  $LiFePO_4$ ,<sup>22</sup> which matched trends that were measured experimentally.<sup>15</sup> In addition, by producing data for hundreds of phosphate chemistries, we observed that phosphates on average have a lower oxidation potential (and thereby higher intrinsic safety) than oxides at the same voltage.<sup>29</sup> However, we also observed that phosphate groups certainly do not guarantee safety, especially at high voltage. In particular, while phosphate safety is often attributed to the difficulty of breaking P–O bonds, we observed that  $O_2$  release can still readily occur by converting one type of polyanion group to another (*e.g.*, by transforming  $PO_4$  groups to  $P_2O_7$  groups).<sup>29</sup>

This work uses high-throughput computation to systematically investigate the effect of redox metal and polyanion group on the voltage and oxidation potential of many types of battery cathodes, including oxides, borates, silicates, phosphates, and sulfates. We report the relationship between voltage and oxidation potential and the effect of chemistry in determining voltage and oxidation potential. Finally, we assess the prospects for designing intrinsically safe, high-voltage cathodes.

## Methods

### Data set

The chemical compounds investigated in this work are ternary and quaternary systems containing Li, one redox-active metal, oxygen, and optionally one of {B, Si, P, S}. We restricted our data to one-electron-or-less redox processes of the metals

{Ti, V, Cr, Fe, Mn, Co, Ni, Cu, Mo}. The compounds originated in either the 2006 Inorganic Crystal Structure Database (ICSD)<sup>30,31</sup> or were predicted compounds based on data-mined algorithms.<sup>32,33</sup>

We excluded compounds with large thermodynamic driving forces for decomposition to other phases, as determined by phase stability diagrams. In particular, this procedure excludes predicted compounds that our computations indicate have a low likelihood for successful synthesis. These phase stability diagrams incorporate calculations on most compounds from the 2006 ICSD<sup>30,31</sup> containing four elements or less. We removed from analysis any cathode material that exhibited over 50 meV per atom instability in the discharged state or over 150 meV per atom instability in the charged state.

The stability filtering procedure reduced 1936 computed compounds to 1409 cathodes used in this study. The number of cathodes for each redox couple/anion pair are plotted in Fig. 1. In general, the ICSD combined with our structure prediction algorithms produce several stable insertion compounds across the entire chemical space. However, several chemistries have few or no compounds. These missing chemistries include  $Cr^{4/5}$ ,  $Cr^{5/6}$ ,  $Mo^{5/6}$ , and  $Cu^{1/2}$  for most polyanions and some redox/polyanion combinations such as  $Mn^{3/4}$  silicates and  $Ni^{3/4}$  in silicates and borates. In most cases, the lack of data in these chemical systems is caused by fewer attempted calculations. However, in some cases (such as  $Ni^{3/4}$  borates,  $Ni^{3/4}$  silicates, and  $Mn^{3/4}$  silicates), several calculations were attempted but we were unable to find many stable compounds. The difference between the number of attempted computations and the number of stable compounds is plotted in the ESI,† Fig. S1.

### DFT computation parameters

The complete details of our high-throughput computational methodology are provided in prior publications;<sup>27,29</sup> we summarize

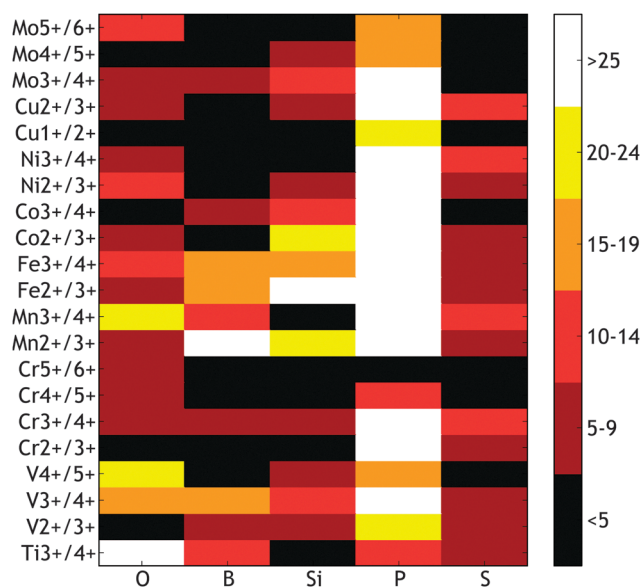


Fig. 1 Number of compounds in the dataset, arranged by redox couple and anion. The 'O' anion group indicates oxides, whereas 'B', 'Si', 'P', and 'S' indicate borates, silicates, phosphates, and sulfates, respectively.

them here. Our computations were performed using the VASP software<sup>34–36</sup> and employed the GGA functional as parameterized by Perdew, Burke, and Ernzerhof.<sup>37,38</sup> To correct self-interaction for compounds containing {Cr, Cu, Co, Fe, Mn, Mo, Ni, V}, we used the rotationally invariant approach to GGA +  $U$  proposed by Dudarev *et al.*<sup>39</sup> and fitted the correction using the method of Wang *et al.*<sup>40</sup> The only exception is the + $U$  for Co (set at 5.7 eV) following Zhou *et al.*<sup>25</sup> When constructing phase diagrams, we used the strategy reported by Jain *et al.*<sup>41</sup> to combine data from GGA and GGA +  $U$  calculated energies. The pseudopotentials and DFT +  $U$  parameters employed in this work are tabulated in the ESI,<sup>†</sup> Table S1.

We initialized all magnetic ions ferromagnetically with high-spin, with the exception of Co-containing compounds which were computed with both high and low spin initializations (with the lowest energy result retained). Additionally, some binary oxides used in phase diagram analysis were computed in their known antiferromagnetic state. We employed an electronic energy convergence cutoff of  $n \times 5 \times 10^{-5}$  eV and an ionic convergence cutoff of  $n \times 5 \times 10^{-4}$  eV along with a  $500/n$   $k$ -point mesh, where  $n$  represents the number of atoms in the unit cell.<sup>27</sup> Each compound was structurally optimized twice in two consecutive runs using the AFLOW software package.<sup>42</sup>

The voltage of a cathode often depends on its state of charge. In most cases, our voltage data represents an average between fully charged and fully discharged states. For multi-electron cathodes, the data is reported separately for each redox couple of the transition metal. However, voltage changes due solely to Li ion ordering effects are not considered. Compounds with partial occupancy of an element on a site were ordered based on reasonable supercell size considerations (generally <100 atoms) and lowest electrostatic energy.<sup>43,44</sup>

The energies of SO<sub>2</sub> and SO<sub>3</sub> gas at room temperature were fit using known experimental reaction energies<sup>45,46</sup> using the method of Wang *et al.*<sup>40</sup> The resulting fit over a variety of sulfate reactions are presented in the ESI,<sup>†</sup> Fig. S2 and S3. However, the behavior of these gases was not modeled as a function of temperature.

We note that it can be difficult to assess the accuracy of computational models. As a guide, and based on a past study of 135 computed reaction energies *versus* experiment using these methods, we expect the standard deviation of error of most computed reaction energies used in constructing phase diagrams to be centered at zero with a standard deviation of approximately 24 meV per atom.<sup>47</sup> For portions of the phase diagram involving mixing delocalized compounds with transition metal compounds, we expect the accuracy of the GGA/GGA +  $U$  mixing strategy to have a mean absolute error of about 45 meV per atom.<sup>48</sup> The expected mean absolute error in voltage calculations (involving redox processes) is approximately 0.2 volts.<sup>26</sup>

### Method for computing oxygen release temperature

To compute an oxygen release temperature, we employ a method introduced in prior publications for calculating the equilibrium oxidation potential ( $\mu_{\text{O}_2}$ ) of compounds as implemented in the pymatgen materials analysis library.<sup>49</sup> This method determines

$\mu_{\text{O}_2}$  by computing phase stability diagrams,<sup>22,23</sup> which indicate the thermodynamically favorable decomposition reaction for O<sub>2</sub> release as well the energy of this reaction for all points in composition space.

By computing  $\mu_{\text{O}_2}$ , we can determine the thermodynamically-driven onset temperature of O<sub>2</sub> gas release. If the chemical potential of oxygen in the environment ( $\mu_{\text{O}_2}^{\text{env}}$ ) is lowered below our computed value of  $\mu_{\text{O}_2}$  for the cathode, there exists a thermodynamic driving force for the system to release oxygen gas by converting to new phases. The external oxygen chemical potential ( $\mu_{\text{O}_2}^{\text{env}}$ ) can be modeled to vary according to temperature and pressure according to the following relation:<sup>22</sup>

$$\mu_{\text{O}_2}^{\text{env}}(T, p_{\text{O}_2}) = H_{\text{O}_2}^0 - TS_{\text{O}_2}^{T, p_0} + kT \ln \frac{p_{\text{O}_2}}{p_0} \quad (1)$$

in which  $H_{\text{O}_2}^0$  corresponds to the O<sub>2</sub> energy at ambient conditions,  $S_{\text{O}_2}^{T, p_0}$  represents the entropy of oxygen gas, and  $p_{\text{O}_2}$  is the ratio of the partial pressure of oxygen gas to that under standard conditions.  $H_{\text{O}_2}^0$  is set to the numerical O<sub>2</sub> energy reported in the previous work of Wang *et al.* that corrects for both binding energy and electronic environment errors.<sup>40</sup> We note that  $H_{\text{O}_2}^0$  also includes the PV term of an ideal gas at ambient conditions. The entropy of oxygen gas as a function of temperature,  $S_{\text{O}_2}^{T, p_0}$ , is taken from experimental data in the NIST Chemistry Webbook.<sup>46</sup> Eqn (1) allows us to convert our computed  $\mu_{\text{O}_2}$  to a thermodynamic onset temperature of O<sub>2</sub> release, assuming that the major temperature dependence comes from O<sub>2</sub> gas entropy alone and not due to temperature-dependent differences in solid phase free energies.

### Comparison of method with experiment and limitations

To assess the relevance of our computed thermodynamic onset temperature as an indicator of cathode safety, we plot in Fig. 2 the relationship between our computed onset temperature and experimentally measured O<sub>2</sub> release onset temperatures for several cathode materials (the raw data is in ESI,<sup>†</sup> Table S2).<sup>15–17,50–63</sup> The relationship between our computed temperature and measured experimental data qualitatively distinguishes the different materials classes (particularly within air or reducing gas environments). It is important to note that the  $p_{\text{O}_2}$  used for the computational prediction is standard conditions (*i.e.* the fit in Wang *et al.*).<sup>40</sup> Quantitative agreement with experiment should not be expected as the experimental  $p_{\text{O}_2}$  is generally not specified or even controlled (*e.g.*, testing in electrolyte or reducing gas, or for electrode materials containing carbon).

At the lowest end of safety are not the oxides but rather Ni and Co phosphate materials. Indeed, both of these materials are speculated to release O<sub>2</sub> at room temperature when fully delithiated.<sup>17,63</sup> For *partially* delithiated LiCoPO<sub>4</sub>, it is worth noting that a study by Okada *et al.*<sup>65</sup> indicated an onset temperature of 200 °C for Li<sub>0.5</sub>CoPO<sub>4</sub>, but actually report a higher onset of 280 °C for Li<sub>0.17</sub>CoPO<sub>4</sub> despite its lower Li content (inconsistent with our computed results and thermodynamic behavior).

Following the delithiated Co and Ni phosphates, the next lowest predicted safety is for charged layered oxides, followed by the

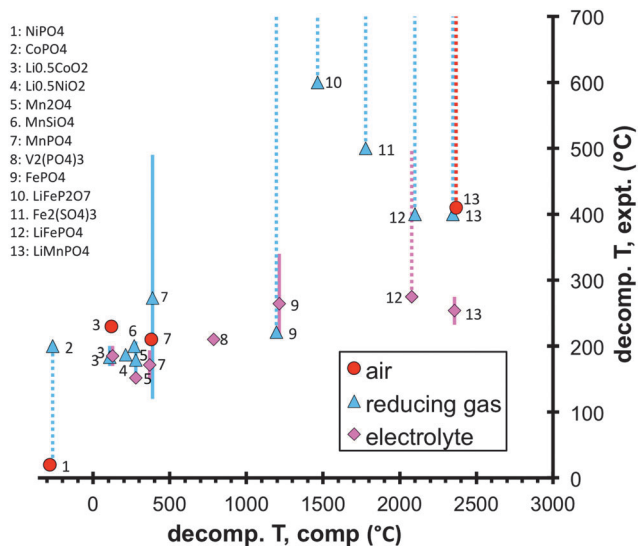


**Fig. 2** Computed versus experimental  $O_2$  gas release temperatures, organized by measurement condition. A small scatter of  $10^\circ C$  was sometimes added to the x-axis to enhance clarity. Experimental values were extrapolated from multiple references.<sup>15–17,50–64</sup> In cases where multiple experimental data were reported for the same compound under the same measurement condition, the average is plotted and the range of reported experimental values is illustrated by a solid two-sided bar. Experimental values with large or undetermined ranges in experimental values are depicted by a dashed one-sided bar, with either a lower-bound or upper-bound plotted. See accompanying text for more details and ESI,<sup>†</sup> Table S2 for the raw data used to compile this chart.

Mn spinel,  $MnSiO_4$ , and  $MnPO_4$ . The experiments are generally consistent with the computed data, with the possible exception of  $MnPO_4$  for which there is considerable disagreement in experimental reports. Data from Chen *et al.*<sup>15</sup> and Kim *et al.*<sup>56</sup> indicate low thermal stability between  $150$ – $210^\circ C$ , whereas data from Martha *et al.*<sup>57</sup> and Choi *et al.*<sup>59</sup> indicate no  $O_2$  release until at least  $300^\circ C$  or  $490^\circ C$ , respectively. Our computations are consistent with the former set of studies.

For compounds with computed  $O_2$  release temperatures above  $1000^\circ C$ , comparison with experiment becomes difficult because experiments generally do not test such high temperatures (for which there are other concerns than  $O_2$  release). The discrepancy between measured experimental values can also be large; for example, the onset of measured  $O_2$  release in  $FePO_4$  in reducing environments ranges from approximately  $220^\circ C$ <sup>51,53</sup> to over  $400^\circ C$ .<sup>15</sup> However, our computed data are consistent with a recent report that  $LiFeP_2O_7$  demonstrates higher thermal stability than  $FePO_4$ .<sup>66</sup>

While our computed  $O_2$  onset temperature is a good general indicator of intrinsic safety, the measure is not expected to be quantitatively accurate. First, the experimental conditions in the different studies are nonuniform, and the reducing environments lower the  $O_2$  onset temperature compared to predicted values at ambient  $O_2$  pressure. Similarly, carbon coatings could further reduce the onset temperature of  $O_2$  release compared to a theoretical value. In ESI,<sup>†</sup> Table S3, we show the degree to which our model would predict different results under different partial pressures of oxygen. For example, a predicted onset of

$500^\circ C$  at atmospheric pressure reduces to  $264^\circ C$  at one-millionth of atmospheric pressure.

Residual Li or overcharging in some of the experiments could also alter  $O_2$  onset. Synthesis method, particle size and shape also play a role in observed  $O_2$  release temperature. Finally, interpreting experimental data is not always trivial, and disagreement in experimental reports can originate from whether observed peaks in differential scanning calorimetry (DSC) or dips in thermogravimetric analysis (TG) represent  $O_2$  release or some other process such as  $H_2O$  liberation or structure transformation.<sup>59</sup> One advantage of the computational approach is that it provides a consistent and well-defined measurement of intrinsic safety.

Despite the qualitative agreement of our computations with experimental data, we mention several limitations of our approach. One limitation is that we only model equilibrium gas evolution; in practice, a compound might release  $O_2$  while in a metastable structure. In some cases, the thermodynamic decomposition path may be very different from the one undertaken in practical operating conditions. In particular, this may be an issue for the compounds that are predicted to release  $O_2$  at very low  $T$ . This possibility is more thoroughly discussed in previous publications.<sup>22,24</sup> A consequence of modeling equilibrium decomposition (but non-equilibrium intercalation) is that we predict different polymorphs of the same composition to possess the same  $\mu_{O_2}$  but different voltages. One justification for this approach is that as temperature increases, metastability becomes less likely; therefore, voltage (relevant for room temperature operation of cells) can involve metastable structures whereas thermal runaway at higher temperatures is less likely to do so.

A second important limitation of our method is that we do not model mixed metal phases such as doped spinels<sup>67</sup> or mixed-metal layered compounds.<sup>54</sup> Our results pertain to mixed metal systems insofar as each metal acts independently of the other. For example, experimental work by Kim *et al.* on mixtures of Mn–Fe olivine materials indicates that decomposition temperatures for mixed systems lie intermediate to the pure metal endmembers.<sup>68</sup> In addition, recent computational work by Hajiyani *et al.* for the olivine system indicates that the critical oxidation potential for mixed metal compounds may lie in between the oxidation potentials of their single metal end members.<sup>69</sup>

Finally, we are only evaluating the conditions at which onset of  $O_2$  evolution from the bulk is expected to occur. We do not model the actual heating rate of the cell due to reaction with the electrolyte, nor do we consider the amount of  $O_2$  evolved. In this respect, our measure is more analogous to TG experiments than DSC experiments.

## Results

### Voltage versus safety

Now that we have established our computational procedure, we report the data for oxidation potentials of 1409 cathode materials representing oxide, borate, silicate, phosphate, and sulfate families (Fig. 3).

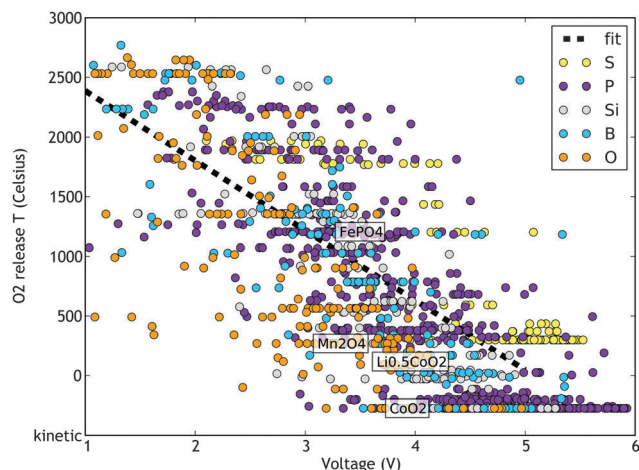


**Fig. 3** Computed voltage versus computed decomposition temperature for 1409 cathodes investigated by high-throughput computation. At very low temperatures, we expect that  $O_2$  release will be limited only by a kinetic barrier rather than by thermodynamics. Several well-known cathodes are indicated on the plot in semitransparent text boxes (the center of the box is at the compound, and the values are also listed in Table S4, ESI†). A linear least-squares fit to the data (excluding points “pinned” at 0 K) is plotted as a dashed line.

The data in Fig. 3 indicates an inverse relationship between voltage and  $O_2$  release temperature, consistent with the previous result from Godshall *et al.* that high voltage cathodes also tend to be less safe.<sup>18</sup> However, we observe considerable scatter in the relation. Excluding points at 0 K in the “kinetic” region, the  $R^2$  value for a linear least-squares fit to the data is 0.53, indicating that almost half of the variance in the  $O_2$  release temperature within our data set can be explained by voltage alone. The other  $\sim 47\%$  of variance is due to other factors. Nevertheless, the correlation illustrates the challenge in designing safe, high-voltage cathodes; as one metric is improved, the other tends to deteriorate.

We note two borate outliers in Fig. 3: at 4.95 V and 2476 °C is  $LiV(B_3O_5)_3$ , and at 5.34 V and 1182 °C is  $LiFe(B_3O_5)_3$ . It is possible that compounds with a  $(B_3O_5)^{-1}$  polyanion group are not accurately modeled by our phase diagrams or by GGA, but we found no reason to exclude these compounds from the study. It should be noted, however, that they have very low maximum theoretical capacity ( $<70$  mA h  $g^{-1}$ ). The sulfate outlier at 5.07 V and 1207 °C is  $LiV(SO_4)_2$ . This compound is not the most stable polymorph and is discussed further later in the text.

While all polyanion chemistries generally exhibit poorer safety with increasing voltage, some polyanions are safer (achieve higher  $O_2$  release temperatures) at a given voltage. For example, the sulfates (yellow) exhibit higher  $O_2$  release temperatures compared to the oxides (orange). To better visualize the difference in voltage versus  $O_2$  release temperature for each polyanion, we separately fit a linear least-squares relation per chemistry and plot the results in Fig. 4. Fig. 4 illustrates that, at a given voltage, safety tends to increase in the order: oxides < silicates < borates  $\sim$  phosphates < sulfates.

Surprisingly, none of the commercial cathodes labeled in Fig. 4 demonstrate extraordinary safety given their voltage and polyanion

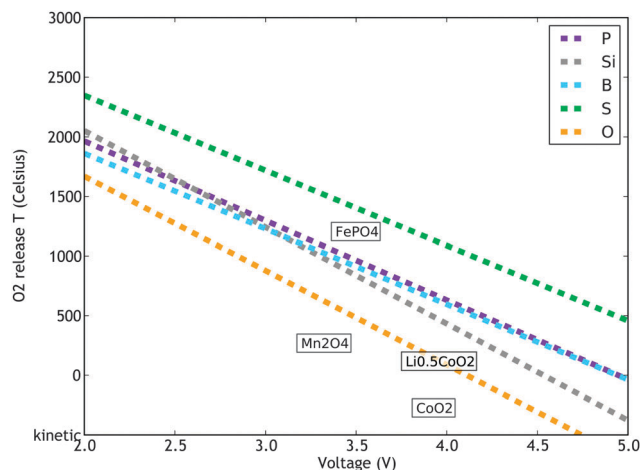


**Fig. 4** Linear-least squares fits to the data presented in Fig. 3, separated by polyanion. Several well-known cathode materials are indicated on the plot in semitransparent text boxes.

chemistry.  $FePO_4$  is only slightly safer than the fitted average for 3.5 V phosphates;  $Li_{0.5}CoO_2$  is approximately as safe as the fitted average for 3.9 V oxides;  $CoO_2$  and  $Mn_2O_4$  are less safe than their fitted averages for oxides. As discussed in later sections, this might be because the compounds that display higher safety at a given voltage often also compromise capacity, which would reduce their commercial viability. The slightly different slopes for the various chemistries can be attributed to the different types of phase diagrams for each chemical system, and in particular the typical reactions leading to  $O_2$  release in each system.<sup>70</sup>

### Effect of redox couple and polyanion type

The type of polyanion group is not the only chemical factor affecting safety. An additional factor determining  $\mu_{O_2}$  is the element and valence state employed for the redox metal.<sup>29</sup> Therefore, we also examine the data in finer detail by plotting the mean voltage and  $O_2$  release temperature for each combination of redox couple/anion type (Fig. 5).

The left panel of Fig. 5 clearly demonstrates the inductive effect; for a given redox couple, voltage increases upon addition of a polyanion group. In addition, polyanions with a highly electronegative cation such as phosphorus and sulfur exhibit the greatest shift in voltage from the oxides, as expected from previous studies.<sup>9</sup> However, the high voltage systems in the left panel of Fig. 5 tend to exhibit the lowest  $O_2$  release temperatures on the right panel (Fig. 5), echoing our results presented in Fig. 3.

The right panel of Fig. 5 demonstrates that the addition of polyanions can actually lower  $O_2$  release temperatures compared to oxides, making them *less* safe than the oxides *at the same redox couple*. The effect is moderate for borates and silicates, but is pronounced for phosphates. The sulfates are computed to be safer than the oxides at low temperatures, but much less safe at high temperatures. It should be repeated, however, that we do not consider the entropic effect of  $SO_2$  and  $SO_3$  gases at high temperature. Our finding that the addition of polyanion group

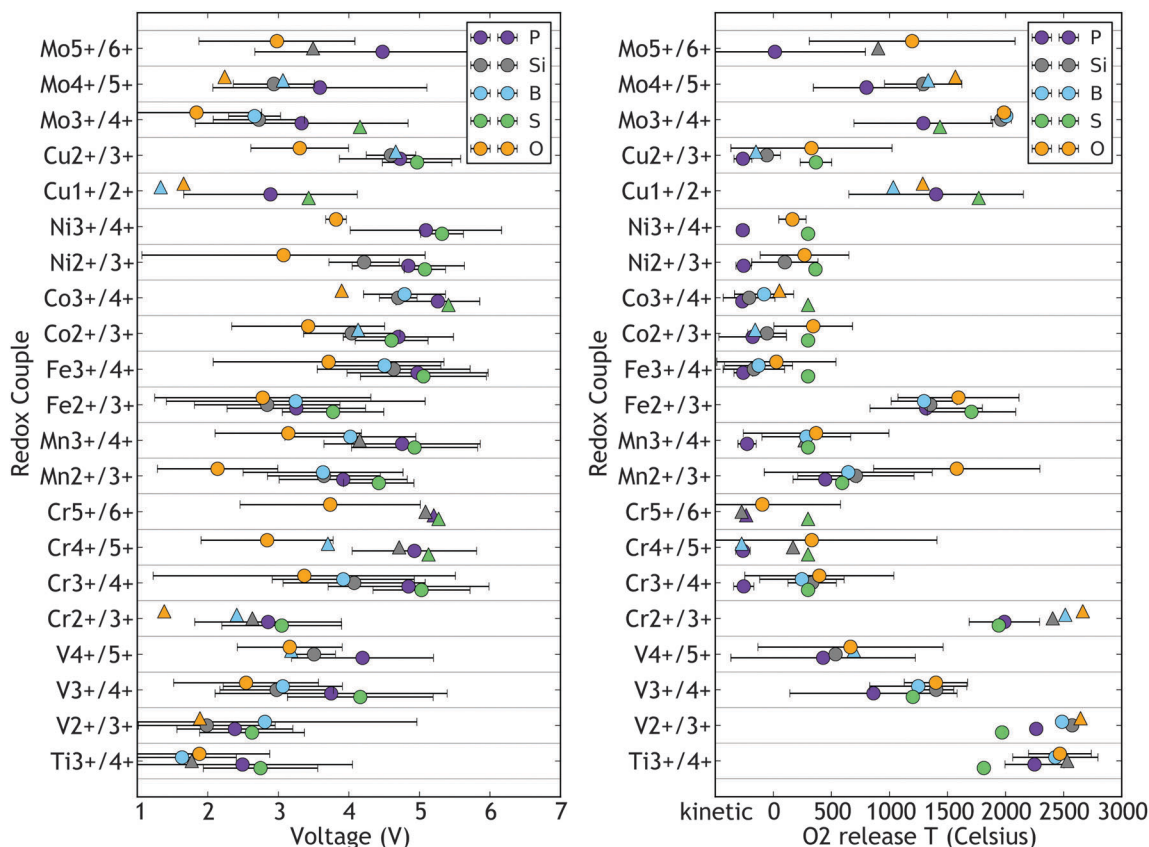


Fig. 5 Voltage (left) and computed O<sub>2</sub> release temperature (right), averaged by redox couple and polyanion and with color corresponding to the anion chemistry. Error bars indicate two standard deviations from the mean value. Points that represent fewer than 5 compounds are denoted by a triangle.

for a fixed redox couple offers no improvement or deteriorates safety is surprising given that polyanions are typically promoted as a route towards high safety.<sup>11,13,14</sup> However, it is consistent with our previous computational data<sup>29</sup> and some experimental data suggesting that Mn<sup>2/3</sup> and Co<sup>2/3</sup> in phosphates is less safe than in oxides,<sup>15,17</sup> although safety data for Mn and Co phosphates is currently still under discussion.

From Fig. 4 and 5, we therefore arrive at two statements regarding the effect of polyanions. At a given *voltage*, polyanions tend to be safer than oxides. However (and counterintuitively), for a given *redox couple*, polyanions exhibit comparable or poorer safety compared to oxides.

### Effect of O/X ratio within polyanion type

Next, we examine whether condensed polyanions (such as PO<sub>3</sub> or P<sub>2</sub>O<sub>7</sub>) might offer better safety at higher voltage compared to polyanions with more oxygen content (such as PO<sub>4</sub> or OPO<sub>4</sub>). Padhi *et al.* have theorized that, neglecting electrostatic factors, condensed phosphates might offer higher inductive effect (and therefore higher voltage) due to shorter P–O bonds that more heavily influence the Fe–O covalency.<sup>71</sup> Indeed, we previously reported that shorter bond lengths and lower O/P ratios resulted in higher voltages in phosphates.<sup>29</sup> Recent work by Tamaru *et al.*<sup>66</sup> also reports the condensed phosphate LiFeP<sub>2</sub>O<sub>7</sub> to be more thermally stable than FePO<sub>4</sub> at a similarly high voltage of 3.52 V

(P<sub>2</sub>/c structure). The Mn analogue LiMnP<sub>2</sub>O<sub>7</sub> also exhibits high voltage and safety, although Li could not be fully extracted from this material and thermal stability was not as high as in LiFeP<sub>2</sub>O<sub>7</sub>.<sup>66</sup> Similar results were also obtained for NaFeP<sub>2</sub>O<sub>7</sub>.<sup>72</sup> These studies encourage us to investigate whether our data also suggests that lower O/X ratios might simultaneously raise voltage and thermal stability.

In Fig. 6, we plot Z-scores of voltage and O<sub>2</sub> release temperature as a function of O/X ratio. For each compound, the Z-score relates either voltage or safety to that of other compounds with the same polyanion chemistry (same cation in the polyanion group) and redox couple:

$$Z_i = \frac{P_i - \mu_{R,X}}{\sigma_X}$$

Here,  $P_i$  is the property of interest for compound  $i$  (either voltage or O<sub>2</sub> release temperature),  $\mu_{R,X}$  is the average value of that property for all compounds with the same redox couple and polyanion counter cation, and  $\sigma_X$  is the standard deviation of the property value for all compounds with the same polyanion counter cation.<sup>29</sup> A Z-score of 1 for  $P =$  voltage thereby indicates that a compound is one standard deviation higher in voltage than compounds with the same redox couple and polyanion element.

We summarize the results of Fig. 6 by polyanion counter element. For borates (blue), the trend is different for O/B ratio

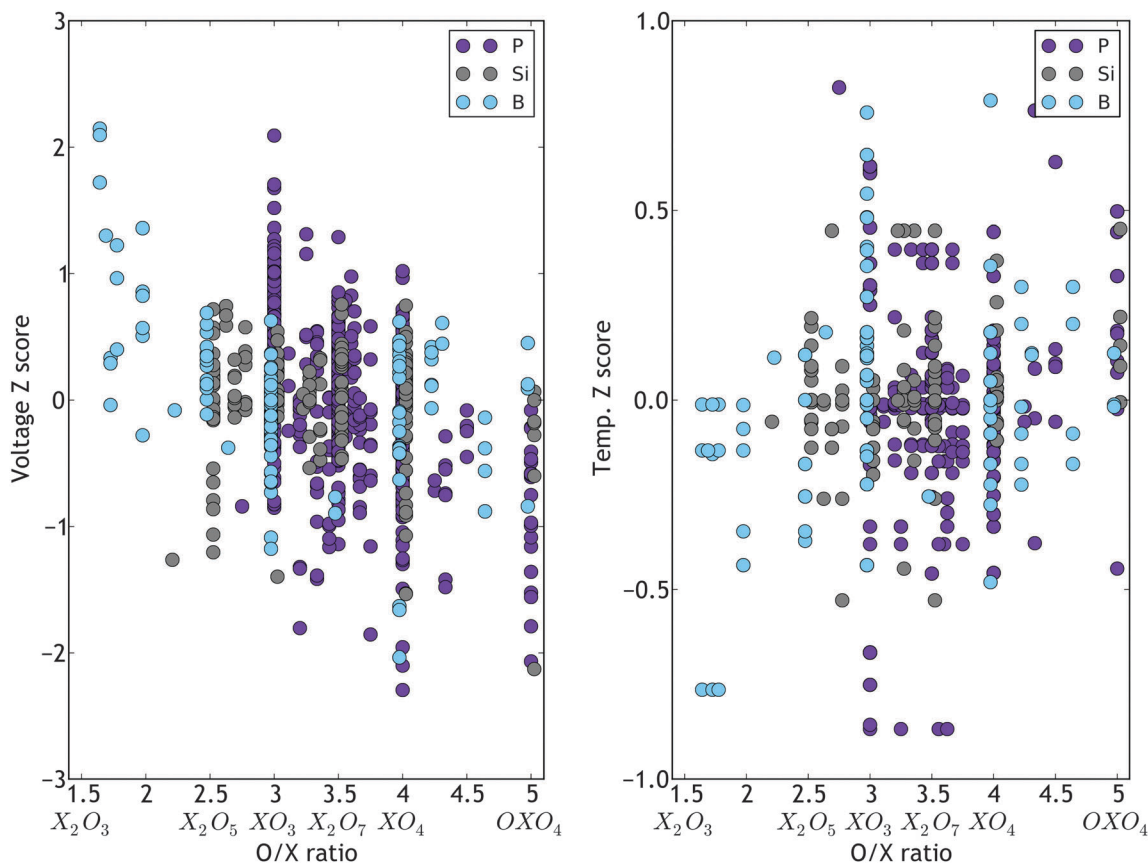


Fig. 6 Voltage (left) and computed  $O_2$  release temperature (right) Z-scores as a function of O/X ratio of the polyanion groups. A small amount of scatter is added to the x coordinate to help distinguish the different polyanions. Data for sulfates is not included because almost all data is for the  $XO_4$  composition.

less than 3 versus for O/B ratio greater than 3. When decreasing the O/B ratio below 3, the voltage increases and thermal stability decreases: the slope and  $R^2$  for a linear least-squares fit to voltage are  $-0.90$  and  $0.53$ , respectively. This indicates that condensing beyond  $BO_3$  greatly increases voltage Z-score. The effect on thermal stability is smaller: a linear least-squares fit to the safety data for  $O/B < 3$  produces a slope of  $0.29$  and  $R^2$  of  $0.21$ . Finally, when increasing the amount of oxygen ( $O/B > 3$ ), the effect is small:  $R^2$  values for both voltage and safety are less than  $0.04$ .

In silicates, we find no evidence that O/Si ratio alone influences properties; a linear least-squares fit produces slopes of less than  $0.1$  and  $R^2$  values of less than  $0.03$  for both voltage and  $O_2$  release temperature.

In phosphates, we find that condensed groups (lower O/P ratios) exhibit higher voltages but do not affect  $O_2$  release temperatures on average. A linear least-squares fit to the data produces a slope of  $-0.55$  and  $R^2$  value of  $0.21$  for voltage, but a slope of less than  $0.02$  and  $R^2$  value less than  $0.001$  for  $O_2$  release temperature. Therefore, condensed phosphates on average provide higher voltages without compromising thermal stability, in support of the experimental and computational results reported by Tamaru *et al.* for the specific case of  $LiMP_2O_7$  ( $M = Fe, Mn$ ) compounds.<sup>66</sup> Unfortunately, this higher

voltage at a given safety generally comes at the cost of lower capacity (see Discussion).

#### Compounds exhibiting high voltage and low intrinsic $\mu_{O_2}$

In addition to examining general trends in voltage versus  $O_2$  release temperature, we examine specific compounds that might possess both high voltage and high intrinsic safety. In Table 1, we list the most stable polymorphs of compounds in our data set that exhibit a voltage greater than  $3.2$  V, a capacity greater than  $100$  mA h  $g^{-1}$ , and have a computed  $O_2$  release temperature over  $1000$  °C, corresponding to thermal stability intermediate to  $Mn_2O_4$  and  $FePO_4$ .

Many of compounds in Table 1 have been previously synthesized and electrochemically tested, such as  $LiVO_2$ ,<sup>73–75</sup>  $LiFeBO_3$ ,<sup>76</sup>  $Li_2FeP_2O_7$  (we note the  $P2_1/c$  polymorph<sup>66</sup> is present in our study, but not the most stable polymorph),<sup>71</sup>  $LiFePO_4$ ,<sup>10</sup>  $Li_2FeSiO_4$ ,<sup>77</sup> and  $Li_2Fe_2(SO_4)_3$ .<sup>78</sup> For  $LiFeSiO_4$ , the computed voltage for the  $Fe^{2/3}$  couple ( $3.28$  V) is close to reported experimental data ( $\sim 3.1$  V).<sup>77</sup> Our calculations indicate that this material should be quite thermally stable as long as the redox couple is restricted to  $Fe^{2/3}$ . However, our calculations also indicate that completely charged  $FeSiO_4$  ( $Fe^{4+}$ ) would possess very low thermal stability and might only be stabilized by kinetic effects. Indeed, fully charged  $FeSiO_4$  (which to our knowledge has not been observed) was filtered from

**Table 1** Compounds with an average voltage higher than 3.2 V, expected decomposition temperature above 1000 °C, and minimum capacity of 100 mA h g<sup>-1</sup>. Only the most stable polymorph(s) of the charged and discharged composition is reported. The columns are formula, voltage (V), computed decomposition temperature ( $T_{\text{crit}}$ ) in Celsius, capacity in indicated formula range (mA h g<sup>-1</sup>), max capacity from charged state assuming usage of all common redox couples (mA h g<sup>-1</sup> max), decomposition energy in meV per atom in charged and discharged states (stab (C) and stab (D)), space group in charged and discharged states (s.g. (C) and s.g. (D)), and unique database id. The ESI lists the crystal structures for these compounds by their unique database id

Formula	Redox	V	$T_{\text{crit}}$	mA h g <sup>-1</sup>	mA h g <sup>-1</sup> (max)	Stab. (C)	Stab. (D)	S.g. (C)	S.g. (D)	Id
<b>Oxides</b>										
Li[0-1]V <sub>3</sub> O <sub>6</sub>	V <sup>3+/4+</sup>	3.65	1354	105	554	129	27	P1	P1	112 705
<b>Borates</b>										
Li[0-1]FeB <sub>5</sub> O <sub>9</sub>	Fe <sup>2+/3+</sup>	4.21	1183	103	103	95	37	P2 <sub>1</sub> /c	P2 <sub>1</sub> /c	136 725
Li[0-1]FeBO <sub>3</sub>	Fe <sup>2+/3+</sup>	3.28	1183	220	220	111	9	Pm	Pm	36 709
Li[3-4]Fe(BO <sub>3</sub> ) <sub>2</sub>	Fe <sup>2+/3+</sup>	3.25	1603	133	133	115	25	P2 <sub>1</sub> 2 <sub>1</sub> 2 <sub>1</sub>	Pnmm	46 569
Li[0-1]VB <sub>5</sub> O <sub>9</sub>	V <sup>2+/3+</sup>	3.21	2476	105	105	115	54	P2 <sub>1</sub> /c	P2 <sub>1</sub> /c	136 409
Li[0-1]VB <sub>2</sub> O <sub>5</sub>	V <sup>3+/4+</sup>	3.48	1028	168	322	93	43	P1	P1	136 521
Li[0-2]V <sub>3</sub> B <sub>3</sub> O <sub>13</sub>	V <sup>3+/4+</sup>	3.67	1354	105	345	147	37	P2 <sub>1</sub> /m	P2 <sub>1</sub> /m	38 176
Li[2-3]V(BO <sub>3</sub> ) <sub>2</sub>	V <sup>3+/4+</sup>	3.23	1291	142	273	139	45	Pc	P2 <sub>1</sub> /c	37 857
<b>Silicates</b>										
Li[0-2]Fe <sub>2</sub> Si <sub>4</sub> O <sub>11</sub>	Fe <sup>2+/3+</sup>	3.35	1351	130	130	95	17	P1	P1	64 538
Li[0-2]Fe <sub>2</sub> Si <sub>5</sub> O <sub>13</sub>	Fe <sup>2+/3+</sup>	3.44	1351	113	113	114	37	P1	P1	60 929
Li[1-2]FeSiO <sub>4</sub>	Fe <sup>2+/3+</sup>	3.28	1358	166	166	102	16	I4	I42m	61 268
Li[3-4]FeSi <sub>2</sub> O <sub>7</sub>	Fe <sup>2+/3+</sup>	3.51	1291	106	106	84	20	P1	C2	57 345
Li[0-2]Mn <sub>3</sub> Si <sub>3</sub> O <sub>10</sub>	Mn <sup>2+/3+</sup>	3.30	1085	127	127	74	20	P1	C2/c	58 704
Li[0-1]V(SiO <sub>3</sub> ) <sub>2</sub>	V <sup>3+/4+</sup>	3.30	1354	128	247	76	4	Pbca	Pbca	63 806
Li[0-1]V(SiO <sub>3</sub> ) <sub>2</sub>	V <sup>3+/4+</sup>	3.24	1354	128	247	70	5	C2/c	P2 <sub>1</sub> /c	133 383
Li[0-1]VSiO <sub>4</sub>	V <sup>3+/4+</sup>	3.26	1354	179	342	116	12	Pbnm	Pbnm	58 385
Li[2-3]VSi <sub>2</sub> O <sub>7</sub>	V <sup>3+/4+</sup>	3.26	1522	112	217	94	30	P1	P1	57 089
<b>Phosphates</b>										
Li[0-2]Cr <sub>3</sub> (P <sub>2</sub> O <sub>7</sub> ) <sub>2</sub>	Cr <sup>2+/3+</sup>	3.61	1892	104	104	107	37	P1	P1	75 918
Li[0-2]Cr <sub>3</sub> (P <sub>2</sub> O <sub>7</sub> ) <sub>2</sub>	Cr <sup>2+/3+</sup>	3.36	1892	104	104	83	37	P1	P1	76 311
Li[1-2]CrP <sub>2</sub> O <sub>7</sub>	Cr <sup>2+/3+</sup>	3.56	2166	112	112	116	38	P2 <sub>1</sub> /c	P2 <sub>1</sub> /c	59 544
Li[0-1]Cu(PO <sub>3</sub> ) <sub>2</sub>	Cu <sup>1+/2+</sup>	3.48	1885	117	117	84	69	P2 <sub>1</sub> /c	P2 <sub>1</sub> /c	78 278
Li[1-2]CuPO <sub>4</sub>	Cu <sup>1+/2+</sup>	3.38	1033	155	155	57	32	Pc	Pmn2 <sub>1</sub>	71 792
Li[1-2]CuPO <sub>4</sub>	Cu <sup>1+/2+</sup>	3.23	1033	155	155	42	37	P2 <sub>1</sub> nb	Pmnb	71 784
Li[0-1]FePO <sub>4</sub>	Fe <sup>2+/3+</sup>	3.42	1205	170	170	20	0	P2 <sub>1</sub> /c	P2 <sub>1</sub> /m	107 637
Li[0-1]FePO <sub>4</sub>	Fe <sup>2+/3+</sup>	3.27	1205	170	170	3	6	Pn2 <sub>1</sub> a	Pn2 <sub>1</sub> a	14 458
Li[0-2]Fe <sub>3</sub> (P <sub>2</sub> O <sub>7</sub> ) <sub>2</sub>	Fe <sup>2+/3+</sup>	3.68	1369	101	101	40	0	P2 <sub>1</sub> /c	P2 <sub>1</sub> /c	12 747
Li[0-4]Fe <sub>5</sub> (P <sub>3</sub> O <sub>11</sub> ) <sub>2</sub>	Fe <sup>2+/3+</sup>	3.27	1205	127	127	33	31	P2 <sub>1</sub> /c	P2 <sub>1</sub> /c	72 124
Li[0-6]Fe <sub>9</sub> (PO <sub>4</sub> ) <sub>8</sub>	Fe <sup>2+/3+</sup>	3.45	1205	123	123	71	48	P1	P1	70 819
Li[1-2]FeP <sub>2</sub> O <sub>7</sub>	Fe <sup>2+/3+</sup>	3.89	1465	110	110	69	3	P1	P1	104 819
Li[1-2]FeP <sub>2</sub> O <sub>7</sub>	Fe <sup>2+/3+</sup>	3.26	1465	110	110	35	24	P1	P1	60 573
Li[0-3]Mo <sub>3</sub> (PO <sub>4</sub> ) <sub>4</sub>	Mo <sup>3+/4+</sup>	3.43	1257	117	227	50	25	P2 <sub>1</sub> /c	P2 <sub>1</sub> /c	159 318
Li[1-3]Mo <sub>2</sub> (PO <sub>4</sub> ) <sub>3</sub>	Mo <sup>3+/4+</sup>	3.55	1346	108	210	83	32	C2/m	C2/m	159 427
Li[0-1]VP <sub>2</sub> O <sub>7</sub>	V <sup>3+/4+</sup>	3.77	1183	116	224	1	0	P2 <sub>1</sub>	P2 <sub>1</sub>	17 334
Li[0-1]VP <sub>2</sub> O <sub>7</sub>	V <sup>3+/4+</sup>	3.34	1183	116	224	0	38	P1	P1	57 975
<b>Sulfates</b>										
Li[0-2]Cr <sub>2</sub> (SO <sub>4</sub> ) <sub>3</sub>	Cr <sup>2+/3+</sup>	3.32	1942	132	132	52	32	Pbca	Pbca	43 205
Li[0-1]CuSO <sub>4</sub>	Cu <sup>1+/2+</sup>	3.57	1769	161	161	43	29	Pn2 <sub>1</sub> a	Pn2 <sub>1</sub> a	135 045
Li[0-1]CuSO <sub>4</sub>	Cu <sup>1+/2+</sup>	3.54	1769	161	161	42	34	R3	R3	135 343
Li[0-2]Fe <sub>2</sub> (SO <sub>4</sub> ) <sub>3</sub>	Fe <sup>2+/3+</sup>	3.69	1778	130	130	9	9	P2 <sub>1</sub> /c	Pbcn	44 300
Li[0-2]Fe <sub>3</sub> S <sub>3</sub> O <sub>13</sub>	Fe <sup>2+/3+</sup>	3.87	1202	110	110	104	49	C2/c	C2/c	134 846
Li[1-2]Fe(SO <sub>4</sub> ) <sub>2</sub>	Fe <sup>2+/3+</sup>	3.89	1778	102	102	27	10	Pc	Pbca	1279
Li[0-1]Ti(SO <sub>4</sub> ) <sub>2</sub>	Ti <sup>3+/4+</sup>	3.41	1813	109	211	86	94	P1	P1	135 054
Li[0-1]V(SO <sub>4</sub> ) <sub>2</sub>	V <sup>3+/4+</sup>	4.38	1201	107	209	3	19	P2/c	C2/m	136 667
Li[0-1]V(SO <sub>4</sub> ) <sub>2</sub>	V <sup>3+/4+</sup>	3.57	1201	107	209	0	84	P1	P1	136 713

our data set due to its large thermodynamic driving force for decomposition to a mixture of Fe<sub>2</sub>O<sub>3</sub>, SiO<sub>2</sub>, and O<sub>2</sub> under ambient conditions. While we know of no experimental thermal stability data on LiFeSiO<sub>4</sub>, experiments have demonstrated that at extreme voltages of 4.7 V (the Fe<sup>3/4</sup> couple) this material is thermally stable until approximately 185 °C.<sup>61</sup>

Three new compounds in the list are potentially interesting as one-electron materials with energy density comparable to LiFePO<sub>4</sub>. The most stable polymorph of LiVB<sub>2</sub>O<sub>5</sub> (id #136521) is

predicted to exhibit a voltage of 3.48 V and has a theoretical capacity of 168 mA h g<sup>-1</sup>, similar to LiFePO<sub>4</sub>. However, both the thermodynamic stability and thermal safety are predicted to be lower than LiFePO<sub>4</sub>. The LiCuSO<sub>4</sub> system (id #135045) is also similar to LiFePO<sub>4</sub> in predicted voltage (3.57 V) and capacity (161 mA h g<sup>-1</sup>). It operates on the unconventional Cu<sup>1/2</sup> redox couple, but is predicted to be reasonably stable from a thermodynamic standpoint and exceeds the predicted thermal safety of LiFePO<sub>4</sub>. Potential issues with Cu<sup>1+</sup>-containing systems are



very different preferred local environments<sup>29</sup> for  $\text{Cu}^{1+}$  and  $\text{Cu}^{2+}$  ions as well as potential mobility<sup>79</sup> of  $\text{Cu}^{1+}$ . However, we note that  $\text{LiCuPO}_4$  was recently synthesized and electrochemically tested with partial reversibility by Snyder *et al.*,<sup>80</sup> thereby encouraging future investigations of  $\text{Cu}^{1/2}$  in chemistries such as sulfates. Finally,  $\text{LiVSiO}_4$  (id #58385) maintains roughly the same energy density as the previous two candidates with a slightly lower voltage (3.26 V) and higher capacity ( $179 \text{ mA h g}^{-1}$ ). This material is predicted to possess extremely high thermal safety (better than  $\text{LiFePO}_4$ ). However, it has a large driving force for thermodynamic decomposition in the charged state (116 meV per atom).

If we expand our search to potential two-electron redox couples by examining the *maximum* capacity listed in Table 1, the number of potential candidates with high theoretical capacities at first appears large. However, it is important to note that all two-electron candidates in the list are based on  $\text{V}^{2-4}$ ,  $\text{Cr}^{2-4}$ ,  $\text{Ti}^{2-4}$ , or  $\text{Mo}^{2-4}$  redox couples. These metals are expected to exhibit a very large voltage step between the  $2+/3+$  and  $3+/4+$  redox couples, with the  $2+/3+$  couple being very low in voltage even in phosphates.<sup>29</sup> Therefore, even if two-electron transfer were achievable, these systems would probably not retain a high voltage for the entire range of intercalation. For example,  $\text{LiVSiO}_4$  (id #58385, mentioned earlier) can potentially exchange 2 electrons *via* the  $\text{V}^{2/3}$  and  $\text{V}^{3/4}$  redox couples, but we expect that the voltage of the  $\text{V}^{2/3}$  couple will be low (most likely under 3 V according to Fig. 5). Similarly,  $\text{LiV}(\text{SO}_4)_2$  (id #136667 in Table 1) has a maximum theoretical capacity of  $208 \text{ mA h g}^{-1}$  for two-electron operation as  $\text{Li}_{0-2}\text{V}(\text{SO}_4)_2$ , but the 4.38 V computation is for the  $\text{Li}_{0-1}\text{V}(\text{SO}_4)_2$  range (we note that another polymorph that is close to 100 meV per atom metastable in the charged state also exists at 5.07 V, *e.g.* see the outlier in Fig. 1). Lithiating  $\text{LiV}(\text{SO}_4)_2$  further to  $\text{Li}_2\text{V}(\text{SO}_4)_2$  would require using the  $\text{V}^{2/3}$  redox couple, which we expect to exhibit a low voltage (between 2.0 to 3.5 V according to Fig. 5).

One exception might be the NASICON-based  $\text{Li}_3\text{Mo}_2(\text{PO}_4)_3$ – $\text{Li}_1\text{Mo}_2(\text{PO}_4)_3$  material, which could use the  $\text{Mo}^{3-5}$  couple within a fairly high voltage range if fully charged to  $\text{Mo}_2(\text{PO}_4)_3$ . We previously suggested that  $\text{Li}_3\text{Mo}_2(\text{PO}_4)_3$  mixed with Fe could make a promising cathode material based on targeted mixing of transition metals.<sup>81</sup>

## Discussion

The design of new cathode materials that exceed the energy density of those currently on the market while retaining safety is a complex optimization problem. The optimization becomes even more complicated as other factors are considered; for example, although nanosizing of electrode particles can enhance rate capability, it can also increase reactivity with the electrolyte and thereby reduce safety.<sup>82</sup>

The two ways to increase energy stored in cathode materials is to increase capacity or to increase voltage. For polyanion systems, increasing the capacity beyond that of the known oxides requires exchanging two-electrons per transition metal.

Materials that can accomplish this feat within a desirable voltage range and without decomposing are extremely rare.<sup>61,83–85</sup> The second method of increasing energy stored, raising the voltage, is attractive because voltage increases not only energy density but also power delivered for a given current density. High-voltage cathodes become essential to high energy density if paired with anodes that are significantly higher in voltage than Li metal, *e.g.*, lithium titanate.

Unfortunately, we find evidence for the general principle first suggested by Godshall *et al.*<sup>18</sup> – that high voltages correlate with lower safety. However, the broader test set investigated in this work reveals that the trend is not as rigid as reported by Godshall *et al.*<sup>18</sup> Some cathode materials have significantly higher safety than others at the same voltage. In particular, at a given voltage, polyanions offer improved intrinsic safety compared to oxides. The best polyanion systems for achieving high voltage and safety are sulfates, followed by the phosphates, borates, and silicates. However, we also observed the unintuitive result that for a given *redox couple*, the polyanion systems demonstrated on average a  $\text{O}_2$  release temperature that was comparable to or worse than oxides.

That the polyanions can exhibit poorer safety for a given redox couple is also consistent with typical oxidation energies of metal oxides *versus* metal polyanion systems. As an example, we compute the energy of  $\text{Mn}_2\text{O}_3$  reduction to  $\text{MnO}$  and  $\text{O}_2$  ( $\text{Mn}^{2/3}$  in oxides) to be  $397 \text{ kJ mol}^{-1}\text{-O}_2$ , whereas the energy of  $\text{MnPO}_4$  reduction to  $\text{Mn}_2\text{P}_2\text{O}_7$  and  $\text{O}_2$  ( $\text{Mn}^{2/3}$  in phosphates) to be only  $150 \text{ kJ mol}^{-1}\text{-O}_2$ . Compared to the oxide, it is much easier to reduce the  $\text{Mn}^{3+}$  to  $\text{Mn}^{2+}$  and form  $\text{O}_2$  gas in the phosphate, leading to a lower  $\text{O}_2$  release temperature.

We found only a few distinct redox couples in our set of compounds in Table 1 screened for high voltage, stability, and safety. These are:  $\text{Fe}^{2/3}$ ,  $\text{Mn}^{2/3}$  (sometimes),  $\text{V}^{3/4}$ ,  $\text{Mo}^{3/4}$  (sometimes),  $\text{Cu}^{1/2}$ ,  $\text{Ti}^{3/4}$  (sometimes), and  $\text{Cr}^{2/3}$ . In Fig. 5, we find little evidence that other redox couples, with the possible exception of  $\text{V}^{4/5}$ ,  $\text{Mo}^{4/5}$ , and  $\text{Mo}^{5/6}$ , could provide both high safety and high voltage. The data in Fig. 5 indicates that some redox couples (such as  $\text{Fe}^{3/4}$ ,  $\text{Cu}^{2/3}$  and Co and Ni systems) are instead quite unlikely to simultaneously possess both a high voltage and intrinsic resistance to  $\text{O}_2$  release.

We observed that using a lower ratio of O/X might increase voltage without adversely affecting safety for  $\text{X} = \text{P}$ . Indeed, several of the high-voltage, high-safety candidates listed in Table 1 are pyrophosphate materials. Although we did not find clear evidence that lowering the O/X ratio is beneficial for the other polyanions, the set of compounds in Table 1 also includes a few condensed borates and condensed silicates. It is important to note, however, that lowering O/X ratios also limits maximum achievable capacity. In a previous publication,<sup>29</sup> we demonstrated that polyanion groups with a large ratio of negative charge-to-mass are capable of the highest theoretical capacities (along with low-valent redox couples, *e.g.*,  $2+/3+$ ). Condensed polyanion groups possess lower anion charge-to-weight ratios and therefore lower capacities. For example, use of the entire  $\text{Fe}^{2/3}$  couple in an orthophosphate (such as  $\text{LiFePO}_4$ ) has a theoretical capacity of  $170 \text{ mA h g}^{-1}$ . However, the same  $\text{Fe}^{2/3}$  redox couple

in a pyrophosphate (such as  $\text{Li}_2\text{FeP}_2\text{O}_7$ ) has a significantly lower theoretical capacity of  $110 \text{ mA h g}^{-1}$ . Therefore, the capacity penalty can be quite severe when using condensed polyanion groups as a route towards safety, although part of this capacity loss should be mitigated by a higher voltage.

In our study, there exist several compounds with high voltage and relatively high safety, but coupled with low thermodynamic stability in the charged state (*i.e.*, close to the 150 meV per atom decomposition energy cutoff employed). It is well known that instability in the charged state leads to high voltages: for example, id #38176 in Table 1 is a  $\text{Li}_2\text{V}_5\text{B}_3\text{O}_{13}$  polymorph with a 147 meV per atom instability in the charged state and a fairly high voltage of 3.67 relative to other  $\text{V}^{3+/4+}$  borates in Fig. 5. However, such charged state instability (with respect to solid phases) might have other side effects, such as cathode decomposition to more stable polymorphs and solid phase mixtures upon cycling.

Overall, our study suggests that the search for both safe and high-voltage cathodes requires designing in a narrow chemical space. To achieve high energy densities with good safety, it might be more practical to address safety concerns by engineering the electrolyte,<sup>86</sup> using alternate electrolytes such as solid state electrolytes or ionic liquids,<sup>87</sup> or by adding surface coatings to cathode particles.<sup>88</sup> We note, however, that our analysis does not include mixed metal systems or assess kinetic barriers to  $\text{O}_2$  release. Alternatively, oxygen-free cathodes based on fluorides or sulfides might avoid the  $\text{O}_2$  release issue altogether, although it is currently uncertain if other detrimental side reactions could occur.

## Conclusion

In this work, we used high-throughput computations on 1409 compounds to systematically investigate the effects of polyanion group, redox metal, and ratio of oxygen to counter cation on voltage and  $\text{O}_2$  release temperature. Overall, we find a strong inverse relationship between voltage and safety that resembles results reported almost 3 decades ago by Godshall *et al.*<sup>18</sup> However, our data indicates that the relationship is not as rigid as that found previously: we find that just over half of the variance in our data set for  $\text{O}_2$  release temperature can be attributed to voltage alone.

We additionally find that safety is higher in polyanion systems compared to oxides for a given voltage. However, we also obtain the non-obvious result that the safety of polyanion systems is comparable to or lower than oxides for a given redox couple. We report a set of compounds that exhibit both high voltage and high  $\text{O}_2$  release temperature in our calculations, but find few general rules for designing safe cathode systems. Condensed phosphates, and to some degree condensed borates, appear to provide higher voltage at comparable thermal stability, but at the cost of limited capacity. Using our data set, we tabulate redox potentials and oxidation potentials for over 105 combinations of redox couple/anion. However, only a few redox couples within a few polyanion systems appear capable of possessing both high voltage and safety. Therefore, safety mechanisms other

than intrinsic cathode resistance to  $\text{O}_2$  release (such as coatings or alternate electrolytes) might be practical alternatives to achieve the goal of designing safe, high voltage Li ion batteries.

## Acknowledgements

The authors would like to acknowledge Bosch and Umicore for funding. Work at the Lawrence Berkeley National Laboratory was supported by the Assistant Secretary for Energy Efficiency and Renewable Energy, under Contract No. DE-AC02-05CH11231. We also acknowledge of the Materials Project<sup>28</sup> database for some of the analysis in this paper through the Department of Energy's Basic Energy Sciences program under Grant No. EDCBEE. In addition, we thank Charles J. Moore for helping perform the calculations in the database and for useful comments, as well as William D. Richardson for contributions to the pymatgen analysis library used in this work.

## References

- 1 Q. Wang, P. Ping, X. Zhao, G. Chu, J. Sun and C. Chen, *J. Power Sources*, 2012, **208**, 210–224.
- 2 National Transportation Safety Board, *NTSB Interim Factual Report DCA13IA037*, 2013.
- 3 D. Doughty and E. P. Roth, *Electrochem. Soc. Interface*, 2012, **21**, 37–44.
- 4 P. Ross, *IEEE Spectrum*, 2013, **50**, 11–12.
- 5 T. M. Bandhauer, S. Garimella and T. F. Fuller, *J. Electrochem. Soc.*, 2011, **158**, R1.
- 6 R. Spotnitz and J. Franklin, *J. Power Sources*, 2003, **113**, 81–100.
- 7 J. W. Fergus, *J. Power Sources*, 2010, **195**, 939–954.
- 8 B. Ellis, K. Lee and L. Nazar, *Chem. Mater.*, 2010, **22**, 691–714.
- 9 M. Arroyo-de Dompablo, M. Armand, J. Tarascon and U. Amador, *Electrochem. Commun.*, 2006, **8**, 1292–1298.
- 10 A. Padhi, K. Nanjundaswamy and J. Goodenough, *J. Electrochem. Soc.*, 1997, **144**, 1188–1194.
- 11 M. S. Islam, R. Dominko, C. Masquelier, C. Sirisopanaporn, A. R. Armstrong and P. G. Bruce, *J. Mater. Chem.*, 2011, **21**, 9811–9818.
- 12 V. Aravindan, K. Karthikeyan, J. W. Lee, S. Madhavi and Y. S. Lee, *J. Phys. D: Appl. Phys.*, 2011, **44**, 152001.
- 13 H. Huang, T. Faulkner, J. Barker and M. Y. Saidi, *J. Power Sources*, 2009, **189**, 748–751.
- 14 A. Yamada and S.-C. Chung, *J. Electrochem. Soc.*, 2001, **148**, A960.
- 15 G. Chen and T. J. Richardson, *J. Power Sources*, 2010, **195**, 1221–1224.
- 16 M. Takahashi, S.-I. Tobishima, K. Takei and Y. Sakurai, *Solid State Ionics*, 2002, **148**, 283–289.
- 17 N. N. N. Bramnik, K. Nikolowski, D. D. M. Trots and H. Ehrenberg, *Electrochem. Solid-State Lett.*, 2008, **11**, A89–A93.
- 18 N. Godshall, I. Raistrick and R. Huggins, *J. Electrochem. Soc.*, 1984, **131**, 543.

- 19 R. A. Huggins, *J. Electrochem. Soc.*, 2013, **160**, A3001–A3005.
- 20 M. Aydinol, A. Kohan, G. Ceder, K. Cho and J. Joannopoulos, *Phys. Rev. B: Condens. Matter Mater. Phys.*, 1997, **56**, 1354–1365.
- 21 G. Ceder, D. R. R. Sadoway, M. K. K. Aydinol, B. Huang, Y.-M. Chiang and Y.-I. Jang, *Nature*, 1998, **392**, 694–696.
- 22 S. P. Ong, A. Jain, G. Hautier, B. Kang and G. Ceder, *Electrochem. Commun.*, 2010, **12**, 427–430.
- 23 S. Ong, L. Wang, B. Kang and G. Ceder, *Chem. Mater.*, 2008, **20**, 1798–1807.
- 24 L. Wang, T. Maxisch and G. Ceder, *Chem. Mater.*, 2007, **19**, 543–552.
- 25 F. Zhou, M. Cococcioni, C. A. Marianetti, D. Morgan and G. Ceder, *Phys. Rev. B: Condens. Matter Mater. Phys.*, 2004, **70**, 1–8.
- 26 V. L. Chevrier, S. P. Ong, R. Armiento, M. K. Y. Chan and G. Ceder, *Phys. Rev. B: Condens. Matter Mater. Phys.*, 2010, **82**, 075122.
- 27 A. Jain, G. Hautier, C. J. Moore, S. P. Ong, C. C. Fischer, T. Mueller, K. A. Persson, G. Ceder and S. Ping Ong, *Comput. Mater. Sci.*, 2011, **50**, 2295–2310.
- 28 A. Jain, S. P. Ong, G. Hautier, W. Chen, W. D. Richards, S. Dacek, S. Cholia, D. Gunter, D. Skinner, G. Ceder and K. A. Persson, *APL Mater.*, 2013, **1**, 011002.
- 29 G. Hautier, A. Jain, S. P. Ong, B. Kang, C. Moore, R. Doe and G. Ceder, *Chem. Mater.*, 2011, **23**, 3495–3508.
- 30 G. Bergerhoff, R. Hundt, R. Sievers and I. D. I. Brown, *J. Chem. Inf. Comput. Sci.*, 1983, **23**, 66–69.
- 31 Inorganic Crystal Structure Database, FIZ Karlsruhe, <http://icsd.fiz-karlsruhe.de/icsd/>.
- 32 G. Hautier, C. C. Fischer, A. Jain, T. Mueller and G. Ceder, *Chem. Mater.*, 2010, **22**, 3762–3767.
- 33 G. Hautier, C. Fischer, V. Ehlacher, A. Jain and G. Ceder, *Inorg. Chem.*, 2011, **50**, 656–663.
- 34 G. Kresse and J. Furthmüller, *Phys. Rev. B: Condens. Matter Mater. Phys.*, 1996, **54**, 11169–11186.
- 35 G. Kresse and J. Furthmüller, *Comput. Mater. Sci.*, 1996, **6**, 15–50.
- 36 J. Hafner, *Comput. Phys. Commun.*, 2007, **177**, 6–13.
- 37 J. Perdew, M. Ernzerhof and K. Burke, *J. Chem. Phys.*, 1996, **105**, 9982.
- 38 J. P. Perdew, K. Burke and M. Ernzerhof, *Phys. Rev. Lett.*, 1996, **77**, 3865–3868.
- 39 S. L. Dudarev, G. A. Botton, S. Y. Savrasov, C. J. Humphreys and A. P. Sutton, *Phys. Rev. B: Condens. Matter Mater. Phys.*, 1998, **57**, 1505–1509.
- 40 L. Wang, T. Maxisch and G. Ceder, *Phys. Rev. B: Condens. Matter Mater. Phys.*, 2006, **73**, 195107.
- 41 A. Jain, G. Hautier, S. P. Ong, C. J. Moore, C. C. Fischer, K. A. Persson and G. Ceder, *Phys. Rev. B: Condens. Matter Mater. Phys.*, 2011, **84**, 045115.
- 42 S. Curtarolo, W. Setyawan, G. L. W. Hart, M. Jahnatek, R. V. Chepulskii, R. H. Taylor, S. Wang, J. Xue, K. Yang, O. Levy, M. J. Mehl, H. T. Stokes, D. O. Demchenko and D. Morgan, *Comput. Mater. Sci.*, 2012, **58**, 218–226.
- 43 P. P. Ewald, *Ann. Phys.*, 1921, **369**, 253–287.
- 44 G. Hart and R. Forcade, *Phys. Rev. B: Condens. Matter Mater. Phys.*, 2008, **77**, 1–12.
- 45 O. Kubaschewski, C. Alcock and P. Spencer, *Materials Thermochemistry*, Pergamon Press, Oxford, 6th edn, 1993.
- 46 P. J. Linstrom and W. G. Mallard, *NIST Chemistry WebBook, NIST Standard Reference Database Number 69*, 2013.
- 47 G. Hautier, S. S. P. Ong, A. Jain, C. C. J. Moore and G. Ceder, *Phys. Rev. B: Condens. Matter Mater. Phys.*, 2011, **75**, 155208.
- 48 A. Jain, G. Hautier, S. P. Ong, C. J. Moore, C. C. Fischer, K. A. Persson and G. Ceder, *Phys. Rev. B: Condens. Matter Mater. Phys.*, 2011, **84**, 045115.
- 49 S. P. Ong, W. D. Richards, A. Jain, G. Hautier, M. Kocher, S. Cholia, D. Gunter, V. L. Chevrier, K. a. Persson and G. Ceder, *Comput. Mater. Sci.*, 2013, **68**, 314–319.
- 50 J. Dahn, E. Fuller, M. Obrovac and U. von Sacken, *Solid State Ionics*, 1994, **69**, 265–270.
- 51 D. MacNeil, Z. Lu, Z. Chen and J. R. Dahn, *J. Power Sources*, 2002, **108**, 8–14.
- 52 A. Yamada, S. C. Chung and K. Hinokuma, *J. Electrochem. Soc.*, 2001, **148**, A224–A229.
- 53 H. F. Xiang, H. Wang, C. H. Chen, X. W. Ge, S. Guo, J. H. Sun and W. Q. Hu, *J. Power Sources*, 2009, **191**, 575–581.
- 54 S. Jouanneau, D. D. MacNeil, Z. Lu, S. D. Beattie, G. Murphy and J. R. Dahn, *J. Electrochem. Soc.*, 2003, **150**, A1299.
- 55 Y. Baba, S. Okada and J. Yamaki, *Solid State Ionics*, 2002, **148**, 311–316.
- 56 S.-W. Kim, J. Kim, H. Gwon and K. Kang, *J. Electrochem. Soc.*, 2009, **156**, A635.
- 57 S. K. Martha, B. Markovsky, J. Grinblat, Y. Gofer, O. Haik, E. Zinigrad, D. Aurbach, T. Drezen, D. Wang, G. Deghenghi and I. Exnar, *J. Electrochem. Soc.*, 2009, **156**, A541.
- 58 A. Veluchamy, C.-H. Doh, D.-H. Kim, J.-H. Lee, H.-M. Shin, B.-S. Jin, H.-S. Kim and S.-I. Moon, *J. Power Sources*, 2009, **189**, 855–858.
- 59 D. Choi, J. Xiao, Y. J. Choi, J. S. Hardy, M. Vijayakumar, M. S. Bhuvaneshwari, J. Liu, W. Xu, W. Wang, Z. Yang, G. L. Graff and J.-G. Zhang, *Energy Environ. Sci.*, 2011, **4**, 4560.
- 60 M. Saïdi, J. Barker, H. Huang, J. L. Swoyer and G. Adamson, *J. Power Sources*, 2003, **119–121**, 266–272.
- 61 T. Muraliganth, K. R. Stroukoff and A. Manthiram, *Chem. Mater.*, 2010, **22**, 5754–5761.
- 62 Q. Wang, J. Sun and C. Chen, *J. Electrochem. Soc.*, 2007, **154**, A263.
- 63 D. Wang, J. Xiao, W. Zu and J.-G. Zhang, *International Meeting on Lithium Batteries*, 2010.
- 64 D. Wang, J. Xiao, W. Zu and J.-G. Zhang, *International Meeting on Lithium Batteries*, 2010.
- 65 S. Okada, M. Ueno, Y. Uebou and J. Yamaki, *J. Power Sources*, 2005, **146**, 565–569.
- 66 M. Tamaru, S. C. Chung, D. Shimizu, S. Nishimura and A. Yamada, *Chem. Mater.*, 2013, **25**, 2538–2543.
- 67 A. Bhaskar, W. Gruner, D. Mikhailova and H. Ehrenberg, *RSC Adv.*, 2013, **3**, 5909–5916.

- 68 J. Kim, K.-Y. Park, I. Park, J.-K. Yoo, J. Hong and K. Kang, *J. Mater. Chem.*, 2012, **22**, 11964.
- 69 H. R. Hajiyani, U. Preiss, R. Drautz and T. Hammerschmidt, *Modell. Simul. Mater. Sci. Eng.*, 2013, **21**, 074004.
- 70 A. Jain, PhD thesis, Massachusetts Institute of Technology, 2011.
- 71 A. K. Padhi, K. S. Nanjundaswamy, C. Masquelier, S. Okada and J. B. Goodenough, *J. Electrochem. Soc.*, 1997, **144**, 1609–1613.
- 72 P. Barpanda, G. Liu, C. Ling, M. Tamaru, M. Avdeev, S.-C. Chung, Y. Yamada and A. Yamada, *Chem. Mater.*, 2013, **25**, 3480–3487.
- 73 L. Zhang, K. Takada, N. Ohta, M. Osada and T. Sasaki, *J. Power Sources*, 2007, **174**, 1007–1011.
- 74 M. M. Thackeray, L. A. de Picciotto, W. I. F. David, P. G. Bruce and J. B. Goodenough, *J. Solid State Chem.*, 1987, **67**, 285–290.
- 75 X. Ma, G. Hautier, A. Jain, R. Doe and G. Ceder, *J. Electrochem. Soc.*, 2012, **160**, A279–A284.
- 76 Y. Dong, Y. Zhao, Z. Shi, X. an, P. Fu and L. Chen, *Electrochim. Acta*, 2008, **53**, 2339–2345.
- 77 A. Nytén, A. Abouimrane, M. Armand, T. Gustafsson and J. O. Thomas, *Electrochem. Commun.*, 2005, **7**, 156–160.
- 78 K. S. Nanjundaswamy, A. K. Padhi, J. B. Goodenough, S. Okada, H. Ohtsuka, H. Arai and J. Yamaki, *Solid State Ionics*, 1996, **92**, 1–10.
- 79 V. Bodenez, L. Dupont, L. Laffont, a. R. Armstrong, K. M. Shaju, P. G. Bruce and J.-M. Tarascon, *J. Mater. Chem.*, 2007, **17**, 3238.
- 80 K. Snyder, B. Raguž, W. Hoffbauer, R. Glaum, H. Ehrenberg and M. Herklotz, *Z. Anorg. Allg. Chem.*, 2014, **640**, 944–951.
- 81 G. Hautier, A. Jain, T. Mueller, C. J. Moore, S. P. Ong and G. Ceder, *Chem. Mater.*, 2013, **25**, 2064–2074.
- 82 J. Yi, C. Wang and Y. Xia, *Electrochem. Commun.*, 2013, **33**, 115–118.
- 83 Q. Kuang, J. Xu, Y. Zhao, X. Chen and L. Chen, *Electrochim. Acta*, 2011, **56**, 2201–2205.
- 84 A. Jain, G. Hautier, C. J. Moore, B. Kang, J. Lee, H. Chen, N. Twu and G. Ceder, *J. Electrochem. Soc.*, 2012, **159**, A622–A633.
- 85 J. Gaubicher, C. Wurm, G. Goward, C. Masquelier and L. Nazar, *Chem. Mater.*, 2000, **12**, 3240–3242.
- 86 B. Mandal, A. Padhi, Z. Shi, S. Chakraborty and R. Filler, *J. Power Sources*, 2006, **161**, 1341–1345.
- 87 M. Armand, F. Endres, D. R. MacFarlane, H. Ohno and B. Scrosati, *Nat. Mater.*, 2009, **8**, 621–629.
- 88 Z. Chen, D.-J. Lee, Y.-K. Sun and K. Amine, *MRS Bull.*, 2011, **36**, 498–505.